RSC Advances

Graphical abstract

Polymeric films based on blends of 6FDA-6FpDA polyimide plus several copolyfluorenes for CO_2 separation.

A. Tena[1,2,4], R. Vazquez-Guilló[3], A. Marcos-Fernández[1,2], A. Hernández[1*], R. Mallavia[3]

[1]*Smap UA-UVA_CSIC, Universidad de Valladolid, Facultad de Ciencias, Real de Burgos s/n, 47071 Valladolid, Spain*

[2]*Instituto de Ciencia y Tecnología de Polímeros, CSIC, Juan de la Cierva 3, 28006 Madrid, Spain*

[3]*Instituto de Biología Molecular y Celular, Universidad Miguel Hernández, 03202, Elche, Alicante, Spain*

[4]*Present address: Helmholtz-Zentrum Geesthacht, Institute of Polymer Research, Polymer Synthesis Dept., Max-Planck-Straße, Geesthacht*

*To whom correspondence should be addressed *tonhg@termo.uva.es*

ABSTRACT

Three emitting copolyfluorenes, based on 2,7-(9,9-dihexyl)fluorene and different aryl groups (1,4-bencene, **PFH-B**; 1,4-bencen-1,2,5-thiadiazole **PFH-BT**; 1,4-naphthalen-1,2,5-thiadiazole, **PFH-NT**), showing diverse acceptor character, in different proportions were blended with a polyimide **6FDA-6FpDA** to make a series of films. These copolyfluorene-polyimide blends were prepared and characterized in solid state, using several techniques. The fluorescence of conjugated polymers can be used as a tool to understand the formation of the membrane and also to increase permeability and selectivity in comparison to films without fluorescence. The relationship between the intrinsic fluorescence of conjugated polyfluorenes and their gas separation properties has been explored in order to establish the influence of the composition and the nature of the aryl group, in the conjugated polymer, on the gas separation performances. In all cases, a low proportion of copolyfluorenes (< 1%weight) gives better CO_2/CH_4 permselectivity properties than the original pure polyimide matrix. The best results were found for the samples that contain PFH-NT. This sample gives 25 % increase in the CO_2 permeability with 15 % increase in CO_2/CH_4 selectivity. Finally, the loss of efficiency in conjugation mechanisms of absorption and emission of the samples could be explained on the basis of the π-staking of the polymer chains produced when a certain low percentage of conjugated polymers in the blend is surpassed. When this π-staking starts, gas permeation properties start to decline too.

1. Introduction

The growing world-wide energy demand causes an increasing interest in exploiting contaminated EOR (enhanced oil recovery) wells as, for example, by using CO_2 injections in miscible-flood-secondary recovery procedures used to rejuvenate mature wells. Moreover global perceptions on climate change are demanding a reduction of carbon emissions. Therefore the gas separation processes for applications in chemical and petrochemical industries are gaining increasing importance[1-3]. The removal of acid gases (such as CO_2) from natural gas, typical pipeline specifications require 2–5% CO_2, is an important process since increases the heating value of natural gas; prevents corrosion of pipeline during gas transport; decreases the volume of gas to be transported in pipelines and reduces atmospheric pollution[4-6]. Therefore, natural gas sweetening – CO_2/CH_4 separation – is increasingly important.

Membrane processes are commercially demonstrated technologies for natural gas processing applications due to their low energy consumption, easy operation and maintenance, environmental friendliness and small footprint, compared to amine absorption, pressure swing adsorption, rectification and cryogenic distillation [7]. In order to have a good gas separation performance, membranes must have high permeability and permselectivity, excellent chemical resistance (for example against corrosive materials such as H_2S), great thermal stability (for high temperature applications), good mechanical properties (for high pressure applications), and good plasticization resistance [8].

Polyimides are well known for their excellent thermal oxidative stability, good organic solvent resistance and exceptional mechanical properties, along with an extraordinary ability of separating complex mixtures of gases in diverse applications [9-11]. Specifically, polyimides with $-CF_3$ groups in their structure produce a restriction of torsional motion of the neighboring phenyl rings that enhances permselectivity. For this reason, one of the most studied polyimides for gas separation is based on 2,2-bis(3,4-dicarboxyphenyl) hexafluoropropane dianhydride (*6FDA*), and the diamine 4,4'-(hexafluoroisopropylidene) dianiline (*6FpDA*) [12-14]. Fully aromatic polyimides have interesting photophysical properties due to both intra- and inter-chain charge transfer interactions [15]. Nevertheless, the four trifluomethyl groups in 6FDA-6FpDA have a

significant electronegativity thus withdrawing electrons and avoiding significant π-bonds, or causing π-stacking and the subsequent quenching of optical activity of the polyimide [16,17].

Among various approaches, the use of polymer blends have been recognized as one of the most cost- and time-effective routes to get good separation properties as they combine the advantages of different materials into a new compound with unique and synergetic properties that are difficult to obtain by other synthesis means [18]. In this way, we explore the possible compatibility and miscibility of blends of polyimides and conjugated polymers. Conjugated polymers are defined as systems connected by π-orbitals with delocalized electrons. One of the most typical conjugated polymers are polyfluorenes and their copolymers, which are a family of blue to red-emitting polymers with large extinction coefficients and great photoluminescence quantum yields[19,20]. Moreover, conjugated polymers are widely used for applications well far away of gas separation[21-24]. For example, they have been used in electronic and photonic devices, showing a great ability and capacity to transfer charge and energy.

Referring to gas separation, copolyfluorenes and 6FDA-6FpDA show accumulation of charges that would give them a clear polar nature leading to dipolar moments that should interact with the intrinsic dipole of the CO_2 molecule. As the CH_4 does not have a relevant polarity, CO_2/CH_4 selectivity should improve.

This paper presents the results obtained for some blends developed from the polyimide 6FDA-6FpDA and several copolyfluorenes (PFH-B, PFH-BT and PFH-NT) in several proportions. Our aim was to correlate the optimal concentration of copolyfluorenes in these blends, for gas separation, with properties of fluorescence that, in turn, give us some clues on their structure.

2. Experimental

2.1. Reagents

All solvents were used as received, without further purification, and were HPLC grade, were purchased from Aldrich Corporation. N,N-Dimethylacetamide (DMAc), chloro(trimethyl)silane (CTMS), pyridine (Py) and ,9-dihexylfluorene-2,7-diboronic acid, 1,4-Dibromobenzene; 1,4-dibromobenzo{2,3}-1,2,5-thiadiazole and tetrakis(triphenylphosphane) palladium(0) were also purchased from Aldrich. Specific reagents such 2,3-diaminonaphthalene was supplied by TCI and 4,4'-(Hexafluoroisopropylidene) diphthalic anhydride (*6FDA*) and 4,4'-(hexafluoroisopro-pylidene)dianiline (*6FpDA*) were acquired from ABCR and sublimed just before use.

2.2. *Synthesis of copolyfluorenes*

The synthesis of the monomers and the cooresponding copolyfluorenes: Copoly-[9,9-bis(n-hexyl) fluorene-*alt*-1,4-bencene] (**PFH-B**); Copoly-[9,9-bis(n-hexyl) fluorene-*alt*-1,4-bencene-1,2,5-thiadiazole] (**PFH-BT**) and Copoly-[9,9-bis(n-hexyl)fluorene-*alt*-1,4-naphthalen-(2,3)-1,2,5-thiadiazole] (**PFH-NT**) are shown in Figure 1. They have been synthesized via the Suzuki coupling reaction, using the same method described in previous studies[25-29].

The required non-commercially available monomers have been synthesized as follows:

- **1,4-dibromo-2,3-diaminonaphthalene** was prepared from 2,3 diaminonaphthalene (12,5mmol) as described in Figure 1 (step i). Here, solid obtained was purified by Versatflash silica column with dichloromethane/hexane mixture (2:1). After evaporation of fractions and drying vacuum at 40ºC overnight gives a white powder (2.08g, 88%).

- **4,9-dibromonaphto{2,3}-1,2,5-thiadiazole**. 1,4- dibromo- 2,3- diaminonaphthalene (0.81g, 2.56mmol) was dissolved in chloroform (25mL) as described in Figure 1 (step ii) and was cooled in an ice bath. Subsequently, a mixture of thionyl chloride (1.27ml, 17.5 mmol), pyridine (3ml) and chloroform (7.6ml) was slowly dropped during 10 minutes. After complete addition the mixture was stirred overnight at 80ºC. Evaporation the solvent and posterior purification in silica with dichloromethane/hexane mixture (3:2) yield an orange solid (564mg, 64%).

Figure 1

In table 1, some characteristics of the new monomers and copolymers synthetized are shown.

Table 1

2.3. Synthesis of the polyimide

Polyimide 6FDA-6FpDA was synthesized by us following the classical in situ silylation two steps method from the 6FDA dianhydride and the diamine 6FpDA, improved by Muñoz et al. [30].

2.4. Blends and Films Preparation

A sketch of the polymers blended is shown in Figure 2a. The copolyfluorenes were added in different percentages 0.1, 1, 5 and 10 % w/w by simple mixing with 6FDA-6FpDA. The membranes were manufactured by using tetrahydrofuran (THF) as solvent. 10% w/v solutions of the blends in THF were prepared and filtered with a 1 mm (Titan, PTFE) membrane. The films were obtained by the method of casting on a leveled glass plate kept at 30 ºC. Afterwards they were kept at 60 ºC during 12 h in order to evaporate most of the solvent. The so-obtained films were separated from the glass by immersion in distilled water and introduced in a vacuum oven at 180 ºC where they were kept during 6 h. The films – some of them are shown in Figure 2b – had a thickness between 35-45 μm.

Figure 2

2.5. Instrumentation

A Thermal Analysis Q500 instrument was used for thermogravimetric analysis (TGA). Disc samples, from 5 to 15 mg, were cut from films and tested. When running dynamic scans, it was done in Hi-Resolution mode, where the heating rate is automatically

adjusted in response to changes in the rate of weight loss, which results in improved resolution, with an initial heating rate of 10ºC/min under a flux of nitrogen.

Differential scanning calorimetry (DSC) analyses were carried out in a Mettler Toledo (DSC 822e) calorimeter equipped with a liquid nitrogen accessory. Disc samples, also weighting 5–15 mg, were sealed in aluminium pans. Samples were afterwards heated at 10ºC/min to each target temperature.

UV absorption spectra were measured with a Shimadzu UV-265FS spectrophotometer. Steady-state emission and excitation spectra were acquired at room temperature using a PTI QuantaMaster Model QM-62003SE spectrofluorometer for different films devices using a solid support well aligned to keep light beams in normal incidence (it is well known that results may vary depending on the angle between the excitation source and detector). Obviously, the signal intensity obtained depends on the optical path, this is why, although the thickness of the samples is very similar, the intensity has been corrected by taking into account the actual thickness of each sample.

2.6. Gas Permeation and selectivity

The permeability, P, for several gases (namely: O_2, N_2, CH_4 and CO_2) was determined by using a permeator with constant volume and variable pressure which uses the ''time-lag'' operation method. Measurements were carried out at 3 bar and 30 ºC. The equations used and the mode of operation of the equipment, as well as an outline of it, has been described previously [31, 32].

3. Results and Discussion

3.1. Characterization of the blends

3.1.1. Thermal stability

TGA results for the synthesized films containing 10% emitting copolyfluorenes and pure 6FDA-6FpDA after being treated at 180 ºC during 6 hours are shown in Figure 3 (similar results are obtained for other percentages).

Figure 3

The initial loss from ambient temperature to 100 ℃, can be attributed to water adsorbed on the sample. A second step approximately from 100 to 250 ℃ is due to water adsorbed into the film along with some residual solvent, with a weight loss from 1 to 1.7%. In the third step the main differences from sample to sample were found. It is worth mentioning that the lowest thermal stability is found for the blend containing PFH-NT which is the most voluminous. In all cases, a comparison with the polymer without presence of copolyfluorene (pure 6FDA-6FpDA) shows that this step cannot be due to an induced degradation of a part of the polyimide structure because, in this range, the degradation for the blends containing copolyfluorene happens at higher temperatures than for the pure polyimide. The final stage of weight loss is due to the thermal decomposition of the remaining aromatic segments. For all copolymers, the residual carbon content at 800 ℃ was around 52 %, with the exception of the blend with PFH-NT residue which was about 46%.

3.1.2.   *Glass transition temperature*

The samples were heated in a DSC instrument with a cyclic method in order to monitor the changes in the thermal properties of the films. First, T_g for the copolyfluorenes were obtained between 120 and 150 °C (116 ℃ for PFH-B, 148 ℃ for PFH-BT, and 149 ℃ for PFH-NT), while for the 6FDA-6FpDA T_g is 287 °C. Then, the analysis was made with the blends with the highest content of the copolyfluorenes (10%). Results confirmed the existence of a single T_g. For the blend with PFH-B T_g it was 279 °C; in the case of the polymer with PFH-BT T_g it was 276 ℃ and finally for the polymer with PFH-NT the value obtained was 278 °C. Obviously all values of blends are below the value of the polyimide 6FDA-6FpDA.

The existence of a single T_g for different blends confirms the complete miscibility of the polymers, as the most extended criterion [33]. One of the major drawbacks when dealing with polymer blends should be a lack of miscibility.

3.1.3.   *Optical properties*

For all the blends with different copolyfluorene concentration, tests of absorption and emission have been performed both in solution and solid state, with insignificant differences. Spectra solutions in tetrahydrofuran (THF) show maximal absorption wavelengths at 230, 390, 445 and 492 nm for 6FDA-6FpDA matrix, PFH-B, PFH-BT and PFH-NT, respectively. These values were used to excite the samples and to register the subsequent emission solid state spectra.

Here, a wide range of emitting wavelengths is covered (PFH-B has a blue emission; PFH-BT shows green emission and PFH-NT emits in red), and furthermore 6FDA-6FpDA matrix gives a transparent film with negligible signals of fluorescence, at the excitation wavelength used. The series of membranes with blends in different ratios have been measured under the same conditions.

A. Copoly-[9,9-bis(n-hexyl) fluorene-alt-1,4-bencene] (PFH-B) blends

The results of emission spectra obtained for the polymer blends derived from 6FDA-6FpDA matrix and PFH-B are shown in Figure 4. The resulting steady-state emission spectra have a shape which is typical of polyfluorenes. It is composed of a 0-0 band centered at 417-421 nm with a vibronic shoulder at 440 nm, assigned to mode 0-1.

Figure 4

The blend with a content of 0.1% in PFH-B, gives low fluorescence signal or intensity, which rises for the 1% blend and remains almost constant for the 5% blend followed by a decrease at 10% content. This quenching effect of the emission is normally found for the blends films of conjugated polymers. PFH-B provides π-type interactions between chains, decreasing the fluorescence intensity, because not all the delocalized electrons in the structure decay to produce fluorescence. Some of these delocalized electrons are being used in interactions with other chain-sites of the same polymer, or with the trifluomethyl groups in 6FDA-6FpDA, with a decrease of the conjugation capacity.

In order to determine the presence and influence of the film on the fluorescence activity of the conjugated polymer (PFH-B in this case), it was extracted by simple solution: one

milligram of membrane was dissolved in 25 ml of THF. Thus, the maximum wavelength (0-0 band/transition) obtained for the pure PFH-B in solution was at 407 nm while 0-1 transition was at 428nm (data not shown). The maximal intensities of fluorescence for the solution test and solid state were compared (insert in Figure 4) where intensities were normalized to the first band with the lowest concentration of polyfluorene (0.1%).

For samples extracted in solution, as expected, the tendency is to increase the intensity when the percentage of polyfluorene is higher. The lack of proportionality is much stronger in the solid state samples, what could be explained as a consequence of concentration and optical pathway effects. In effect, the reduction of the intensity of fluorescence for polyfluorene contents over 0.1 % could be caused by low thickness or self-absorption of high-energy photons [34].

B. *Copoly-[9,9-bis(n-hexyl)fluorene-alt-1,4-bencene-1,2,5-thiadiazole] (PFH-BT) blends*

The insertion of a benzothiadiazole (BT) group into the copolyfluorene structure provides an acceptor of electron charge that acts as a powerful excitation trap. In fluorene copolymers, the addition of BT in the main chain (*PFH-BT*) produces a quenching of the blue emission of the fluorene units, as compared to that seen in the films of PFH-B blends, due to the efficient excitation energy transfer from fluorene to the BT ring [35]. Moreover, in analogous polyfluorene derivatives containing BT, their photoluminescence promotes strong dipole–dipole coupling, and nearly complete quenching of the blue luminescence [36, 37].

Figure 5 shows the emission spectrum obtained for the blends containing PFH-BT copolyfluorenes with different weight proportions. The incorporation of the BT group enhances the fluorescence and causes the appearance of a broad fluorescence band in the range of 535-550 nm for the sample with a very low content of copolyfluorene (0.1%). Furthermore, an increase of emission intensity was registered from 0.1% to 1% weight of PFH-BT blends while for 5 and 10% blends the emission decreased. The maximum intensity obtained was founded for the blends with 1% of PFH-BT copolymer. Possibly, with a 5% of conjugated polymer the effect of auto-quenching due

to interaction between chains appeared. For the sample with 10% the effect was even more pronounced. Here, high concentration of conjugated polymer in the bulk matrix produces a stabilization of the intra- or inter-molecular charge transition state because torsion is not possible anymore. This has been previously described, in an oligomer of fluorene-dibenzothiophene-S,S-dioxide (FSF) dispersed in a Zeonex matrix [38].

Figure 5

The maximum wavelength emission for solutions of extracted conjugated polymer in THF solution was at 538 nm. Like for the PFH-B blends, it was observed that the samples in solution (1 mg of blend / 25 ml THF) have much higher relative intensities than the film samples. In solid state, the blend 6FDA-6FpDA/PFH-BT 1% showed the greatest electron delocalization.

C.   *Copoly-[9,9-bis(n-hexyl)fluorene-alt-1,4-naphthalen-(2,3)-1,2,5-thiadiazole]*
        (PFH-NT) blends

The naphthodithiadiazole (NT) group increases red-emission due to its extended conjugation length, with any strong donor group in the copolymer structure leading to a possible suppression of intermolecular dipole-dipole interactions[28]. This group produces an increase in emission with respect to the BT group due to its intrinsic planar character and different π-stacking interaction in the films. Figure 6 shows the emission spectrum obtained for the 6FDA-6FpDA/PFH-NT blends.

Figure 6

In this case, the maximum intensity appears for the blends with 5% of PFH-NT polymer. For the polymer with a 10 % of polyfluorene, the quenching effect between chains is significant, producing a strong decrease of the peak intensity, probably due to the same stabilization of inter-molecular charge transition above commented, but appearing now for larger concentrations.

It was observed for the solution samples (1 mg / 25 ml THF) that the maximum emission wavelength of pure conjugated polymer appears at 618 nm, corresponding in

this case, with the value for the sample with 5% weight of PFH-NT. The relation between the fluorescence intensity for the films and the solutions can indicate that there aren't any influence in the interaction between the chains for blends until a proportion of 5% of copolyfluorene (see insert in Figure 6). Again, the variation observed at higher percentages may be produced by hindering of chain torsion and stabilization of the inter-molecular charge transition state. This explanation agrees with the red-shift wavelength (5nm) observed for 10% blend with respect to 5% one and around 10 nm, when the content of PFH-NT increased from 0.1 to 5 % (Figure 7). This phenomenon normally is produced when surrounding produces a collapse or π-stacking of the chains and/or could be due to the appearance of a new preferred orientation produced by the planar effect of the naphthalene group into films [39]. These results for PFH-NT blends are promising and suggest that they should have influence on the permselectivity of the membrane.

It is worth noting that there is a clear red-shift of the maximum wavelength for increasing percentages of all polyfluorenes that can be observed in Figures 4 to 6 and is shown in Figure 7. This phenomenon can be attributed to low wavelength quenching as mentioned.

Figure 7

3.2.Permeation properties

3.2.1. Permeability and selectivity

The evolution of permselective properties of the films are certainly influenced by the amount of copolyfluorene in the blend. Figure 8a shows the CO_2 permeability obtained for the samples.

Pure polyimide films show lower permeability than the blend membranes with low content of conjugated polymers PFH-BT and PFH-NT probably due to the voluminous character of the corresponding groups. This is not the case for the blends containing PFH-B that for equally low percentages of copolyfluorene have permeabilities quite

similar to those of the pure polyimide. Actually all the copolymers have similar permeabilities over those of the pure 6FDA-6FpDA for percentages over 0.1 % to 3 %. Over this percentage all the blends give lower permeabilities.

The decrease of permeability for high copolyfluorene contents could be attributed to two effects. This type of conjugated polymer containing charge transfer complexes (CTC), produces quenching that can be attributed to the interaction of π electrons of the aromatic rings in the structures of the polymers[40]. This causes a minimization of charge delocalization along the polymer chain thus decreasing chain-to-chain repulsion and decreasing both polarity (solubility of polar species) and free volume (diffusivity). Then both solubility and diffusivity would decrease for increasing amounts of polyfluorenes. The initial increase of permeability for low polyfluorene contents could be attributed to initial repulsion of delocalized charges with initial increases in free volume and polarity.

Figure 8b shows the results of CO_2/CH_4 selectivity as a function of the percentage of polymers in the blend. As in the previous case, it is observed that for contents over 2%, the selectivity results for this couple of gases are below those of the pure polyimide for the blends containing PFH-BT and PFH-B while selectivities over those of the pure polyimide are obtained up to 5% of copolyfluorene in the case of PFH-NT. The blends containing PFH-BT show selectivities quite similar to those of the pure 6FDA-6FpDA for very low percentages of the copolyfluorene. In any case, low percentages of polyfluorene show the best results. The improvement is substantial for example in the case of the blend with a 1% of PFH-NT copolymer. These improvements of selectivity, show that there should be some kind of favorable interaction with CO_2, which do not affect CH_4, probably due to their different polarities, hence the selectivity increases.

> **Figure 8**

In summary, results show that both the permeability and the selectivity improve with respect to the pure polyimide for percentages of polyfluorene around 1 % with ulterior deterioration of both the properties for percentages over 3%. Is seems also clear that the variation of these properties with the percentage of polyfluorene is strongly influenced by the type of polymer conjugate used for the formation of the blend. The highest

relative improvement was found for PFH-NT. In this case, permeability improves more than 23% over that of the initial polymer, while selectivity increases 15% over the pure polyimide results. It is clear that optimal polyfluorene contents are around 1% when they show the best balance between permeability and selectivity enhancements. In addition, the percentage of rise depends on the type of polyfluorene.

A visual way of representing the permselective properties obtained for different gases are the Robeson's representations [41, 42]. In these representations the distance to the so called upper bond gives us an idea of the permeation properties of the samples. In Figure 9 the Robeson's plot for the CO_2/CH_4 pair is shown.

> **Figure 9**

3.2.2. Diffusivity and solubility

Figure 10 shows the results of solubility and diffusivity for PFH-NT polymer blends. It is seen that diffusivity changes only slightly with a maximum value for blends containing 0.1 % of polyfluorene and decreasing slowly for increasing percentages. In turn solubility is maximal for 1 % polyfluorene in the blend and decreases strongly for increasing contents. This seems to indicate that solubility should play the key role in the decrease of permeability for increasing polyfluorene contents.

> **Figure 10**

3.2.3. Correlation of permeation and fluorescence

In Figure 11 we present the improvement in permeability and selectivity over those of the pure polyimide as a function of the relative intensity of fluorescence in the solid state, I_S, as compared to that in solution, I_L, for the blends containing PFH-NT (similar results are obtained for the other copolyfluorenes. It seems clear that when fluorescence is not affected by quenching (i.e. when the chain-chain structures induced by delocalized electrons are preserved) the fluorescence intensity in the solid state is more similar to that in solution leading to higher permeability and selectivity. In these

conditions the CO_2 interactions with the π electrons of the aromatic rings and the free volume effect of the voluminuous polyfluorenes have maximum effects.

```
Figure 11
```

4. Conclusions

A series of new blends have been prepared. These polymer blends have been synthesized by the simple mixture between a polyimide (6FDA-6FpDA), and different conjugated polymers (copolymers copoly-[9,9-bis(n-hexyl) fluorene-*alt*-1,4-bencene] (PFH-B), copoly-[9,9-bis(n-hexyl) fluorene-*alt*-1,4-bencene-1,2,5-thiadiazole] (PFH-BT), and copoly-[9,9-bis(n-hexyl) fluorene-*alt*-1,4-naphthalen-(2,3)-1,2,5-thiadiazole] (PFH-NT)) in several proportions.

TGA analysis informed about the stability of the mixtures of the polyimide and the chromophore polymers at the treatment temperature. DSC probed that there was a unique T_g for the blends, confirming the fully miscibility of the blends. It was determined that the T_g were between the values of the pure polyimide and the polyfluorenes.

The comparison between the intensities of the samples in solid state and polymers in solution gave us information about the state of the polyfluorenes in the films. It was observed that above 5% polyfluorene content the polymers showed quenching effect, losing effectiveness in fluorescence. The analysis of the maximum showed a red-shift when the percentage of fluorophore polymer in the blend increases, again due to the effect of the interactions with the medium.

The best permeselectivity was found for the blends with low fluorene content. The samples with a content lower than 5% of conjugated polymers showed permeabilities and selectivities better than the pure polyimide. CO_2 permeability reaches improvements over 23 % and CO_2/CH_4 selectivity reached almost 15 % enhancement. Especially good results are got for the PFH-NT blends.

The solubility of the samples with a 0.1 and 1% content increase despite the diffusivity remains almost constant. This could be attributed to the polarity of the copolyfluorene molecules that is high to increase the CO_2 solubility but not so high, if the copolyfluorene content is kept low enough, as to allow significant chain-to-chain structuration and loss of fluorescence due to quenching.

To sum up, it seems clear that this type of modification by the formation of polymer blends with conjugated polymers is suitable for separations where CO_2 is involved, and especially for the separation CO_2/CH_4. This separation has a great importance in the processing of the natural gas. The simplicity of blending makes these materials an attractive alternative to the current polymeric materials for these applications.

5. Aknowledgements

6. *References*

1. F. Ahmad, K. K. Lau, A. M. Shariff and G. Murshid, *Computers and Chemical Engineering*, 2012, **36**, 119-128.
2. A. Hart and N. Gnanendran, *Energy Procedia*, 2009, **1**, 697-706.
3. F. G. Kerry, *Industrial Gas Handbook: Gas Separation And Purification*, CRC Press, 2007.
4. R. W. Baker, *Industrial & Engineering Chemistry Research*, 2002, **41**, 1393-1411.
5. B. D. Bhide, A. Voskericyan and S. A. Stern, *Journal of Membrane Science*, 1998, **140**, 27-49.
6. Y. Xiao, B. T. Low, S. S. Hosseini, T. S. Chung and D. R. Paul, *Progress in Polymer Science*, 2009, **34**, 561-580.
7. P. Bernardo, E. Drioli and G. Golemme, *Industrial and Engineering Chemistry Research*, 2009, **48**, 4638-4663.

8. C. A. Scholes, S. E. Kentish and G. W. Stevens, *Recent Patents on Chemical Engineering*, 2008, 52-66.

9. M. I. Bessonov, M.M. Koton, V.V. Kudryavtsev and L.A. Laius, *Polyimides: Thermally Stable Polymers*, Plenum, New York, USA, 1987.

10. M. K. Ghosh and K.L. Mittal, ed., *Polyimides: Fundamentals and Applications*, Marcel Dekker, New York, USA, 1996.

11. D. S. Wilson, H.D. Stenzenberger and P.M. Hergenrother, eds., *Polyimides*, Blackie, Glasgow, UK, 1990.

12. M. Das and W. J. Koros, *Journal of Membrane Science*, 2010, **365**, 399-408.

13. A. Tena, L. Fernández, M. Sánchez, L. Palacio, A. E. Lozano, A. Hernández and P. Prádanos, *Chemical Engineering Science*, 2010, **65**, 2227-2235.

14. R. Wang, C. Cao and T.-S. Chung, *Journal of Membrane Science*, 2002, **198**, 259-271

15. M. Hasegawa and K. Horie, *Progress in Polymer Science*, 2001, **26**, 259-335.

16. C. A. Hunter and J. K. M. Sanders, The nature of π-π interactions, Journal of the American Chemical Society, 1990, **112** (14), 5525-5534.

17. S.E. Wheeler and J. W. G. Bloom, Toward a More Complete Understanding of Noncovalent Interactions Involving Aromatic Rings, J. Phys. Chem. A, 2014, **118**, 6133−6147

18. L. M. Robeson, *Polymer Blends: A Comprehensive Review*, Hanser Gardener Publications, Cincinnati, OH, 2007.

19. M. Leclerc, *Journal of Polymer Science, Part A: Polymer Chemistry*, 2001, **39**, 2867-2873.

20. U. Scherf and E. J. W. List, *Advanced Materials*, 2002, **14**, 477-487.

21. C. L. Chochos and S. A. Choulis, *Progress in Polymer Science*, 2011, **36**, 1326-1414.

22. A. C. Grimsdale, K. L. Chan, R. E. Martin, P. G. Jokisz and A. B. Holmes, *Chemical Reviews*, 2009, **109**, 897-1091.

23. M. J. Tapia, M. Montserín, A. J. M. Valente, H. D. Burrows and R. Mallavia, *Advances in Colloid and Interface Science*, 2010, **158**, 94-107.

24. C. Zhu, L. Liu, Q. Yang, F. Lv and S. Wang, *Chemical Reviews*, 2012, **112**, 4687-4735.

25. B. Liu and G. C. Bazan, *Nature Protocols*, 2006, **1**, 1698-1702.

26. R. Mallavia, F. Montilla, I. Pastor, P. Velásquez, B. Arredondo, A. L. Álvarez and C. R. Mateo, *Macromolecules*, 2005, **38**, 3185-3192.

27. R. Molina, S. Gómez-Ruiz, F. Montilla, A. Salinas-Castillo, S. Fernández-Arroyo, M. Del Mar Ramos, V. Micol and R. Mallavia, *Macromolecules*, 2009, **42**, 5471-5477.

28. P. Wei, L. Duan, D. Zhang, J. Qiao, L. Wang, R. Wang, G. Dong and Y. Qiu, *Journal of Materials Chemistry*, 2008, **18**, 806-818.

29. J. Yang, C. Jiang, Y. Zhang, R. Yang, W. Yang, Q. Hou and Y. Cao, *Macromolecules*, 2004, **37**, 1211-1218.

30. D. M. Muñoz, J. G. de la Campa, J. de Abajo and A. E. Lozano, *Macromolecules*, 2007, **40**, 8225-8232.

31. A. Tena, A. Marcos-Fernández, A. E. Lozano, J. G. de la Campa, J. de Abajo, L. Palacio, P. Prádanos and A. Hernández, *Journal of Membrane Science*, 2012, **387–388**, 54-65.

32. A. Tena, A. Marcos-Fernandez, L. Palacio, P. Cuadrado, P. Pradanos, J. De Abajo, A. E. Lozano and A. Hernandez, *Industrial & Engineering Chemistry Research*, 2012.

33. D. R. Paul and S. Newman, *Polymer blends*, Academic Press, USA, 1978.
34. J. R. Lakowicz, *Principles of Fluorescence Spectroscopy*, Springer, 2006.
35. Z. Ma, S. Lu, Q.-L. Fan, C.-Y. Qing, Y.-Y. Wang, P. Wang and W. Huang, *Polymer*, 2006, **47**, 7382-7390.
36. J. Chappell, D. G. Lidzey, P. C. Jukes, A. M. Higgins, R. L. Thompson, S. O'Connor, I. Grizzi, R. Fletcher, J. O'Brien, M. Geoghegan and R. A. L. Jones, *Nature Materials*, 2003, **2**, 616-621.
37. E. B. Namdas, T. D. Anthopoulos, I. D. W. Samuel, M. J. Frampton, S. C. Lo and P. L. Burn, *Applied Physics Letters*, 2005, **86**, 1-3.
38. F. B. Dias, S. King, A. P. Monkman, I. I. Perepichka, M. A. Kryuchkov, I. F. Perepichka and M. R. Bryce, *The Journal of Physical Chemistry B*, 2008, **112**, 6557-6566.
39. R. Traiphol, N. Charoenthai, T. Srikhirin, T. Kerdcharoen, T. Osotchan and T. Maturos, *Polymer*, 2007, **48**, 813-826.
40. R. A. Dine-Hart and W. W. Wright, *Makromolecular chemistry*, 1972, **153**, 237.
41. L. M. Robeson, *Journal of Membrane Science*, 1991, **62**, 165-185.
42. L. M. Robeson, *Journal of Membrane Science*, 2008, **320**, 390-400.

Figures

Figure 1.   Synthetic approach of PFH-B, PFH-BT and PFH-NT: i) Br_2 /AcOH, RT, 3h (87%); ii) $SOCl_2$, Pyr, $CHCl_3$; 80ºC, overnight (64%); iii) K_2CO_3, [$Pd(PPh_3)_4$], THF/H_2O, 85ºC, 48h.

Figure 2.   Chemical structure of the polymers used here (a) and the films obtained (b).

Figure 3.   TGA curves in dynamic conditions for the blends with the highest percentage of copolyfluorene and the pure 6FDA-6FpDA without any copolyfluorene.

Figure 4.   Emission spectra for 6FDA-6pDA/PFH-B films at different percentages (λ_{exc} = 390 nm). Insert: Normalized emission intensity as a function of the percentage of PFH-B in the blend.

Figure 5.   Emission spectra for 6FDA-6pDA/PFH-BT films at different percentages (λ_{exc} = 445 nm). Insert: Normalized emission intensity as a function of the percentage of PFH-BT in the blend.

Figure 6.   Emission spectra for 6FDA-6pDA-PFH-NT films at different percentages (l_{exc} = 492 nm). Insert: Normalized emission intensity as a function of the percentage of PFH-BT in the blend.

Figure 7.   Redshift of the emission spectrum versus polyfluorene content.

Figure 8. CO_2 permeability (a) and CO_2/CH_4 selectivity (b) as a function of the copolyfluorene in the blend. Lines are only for eye-guiding and have been extrapolated asymptotically to 0 % of polyfluorene.

Figure 9.   Robeson 's plot for CO_2/CH_4.

Figure 10. CO_2 solubility and diffusivity as a function of the percentage of PFH-NT in the blends.

Figure 11.   Percentage of increment of CO_2 permeability (a) and CO_2/CH_4 selectivity (b) as a function of fluorescence intensity in the solid state referred to that in liquid state (solid state quenching).

Tables

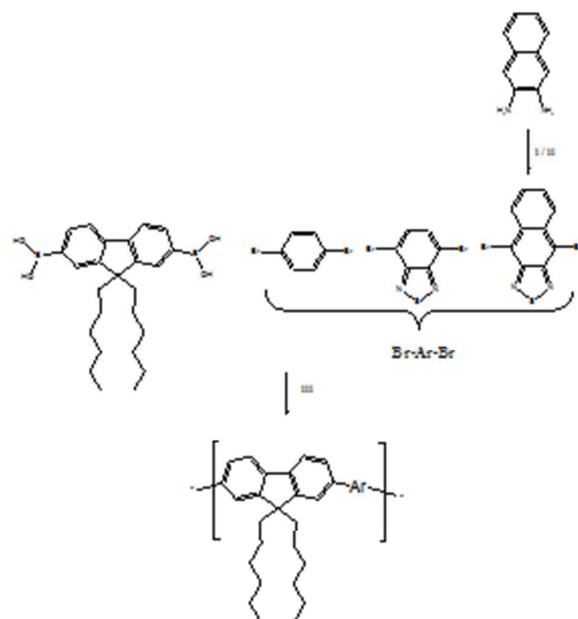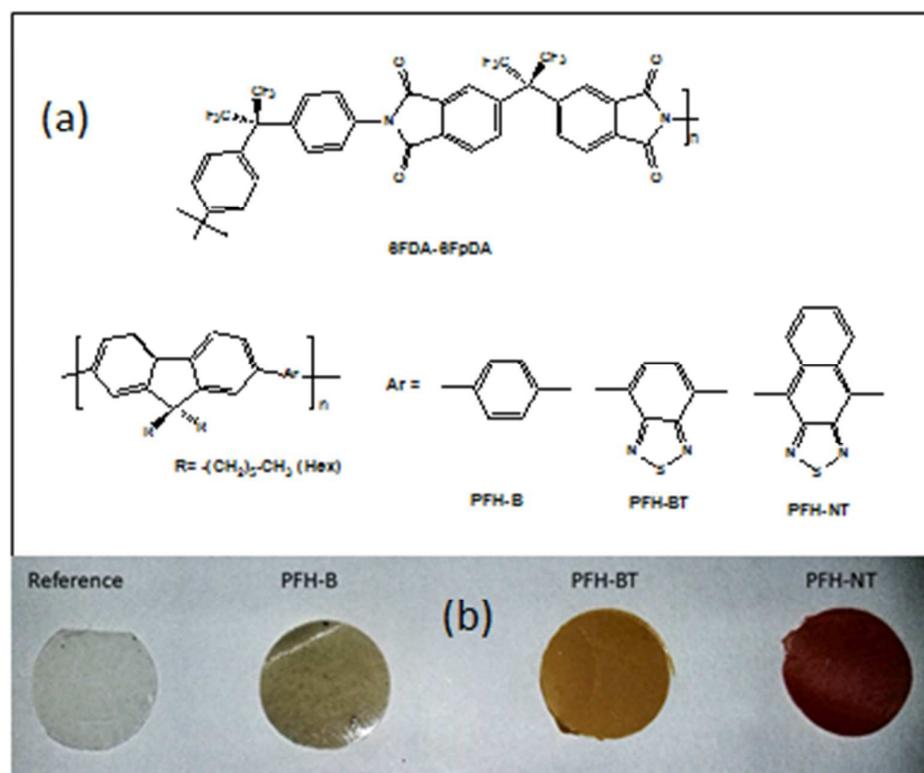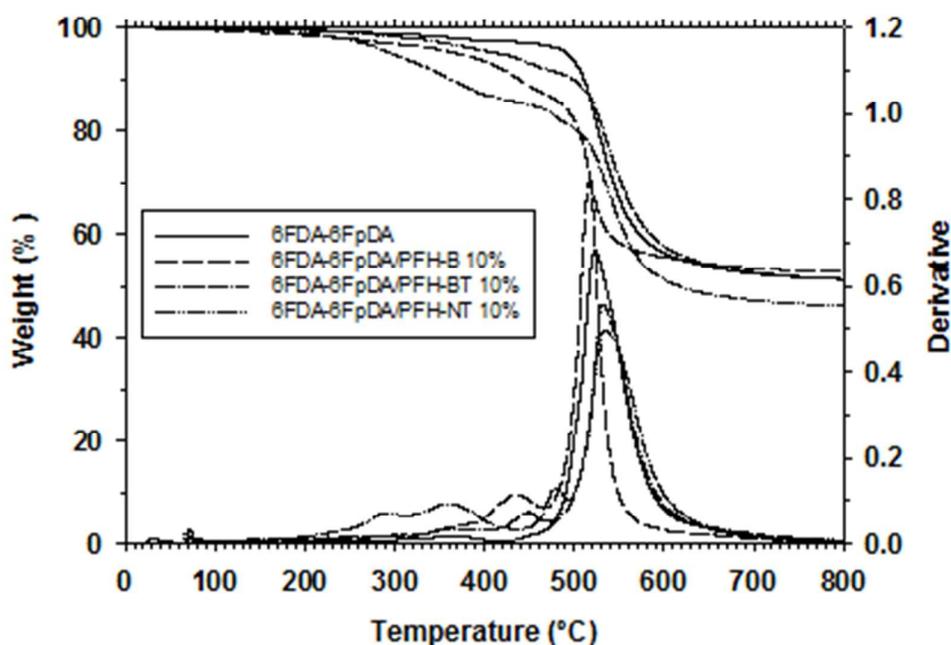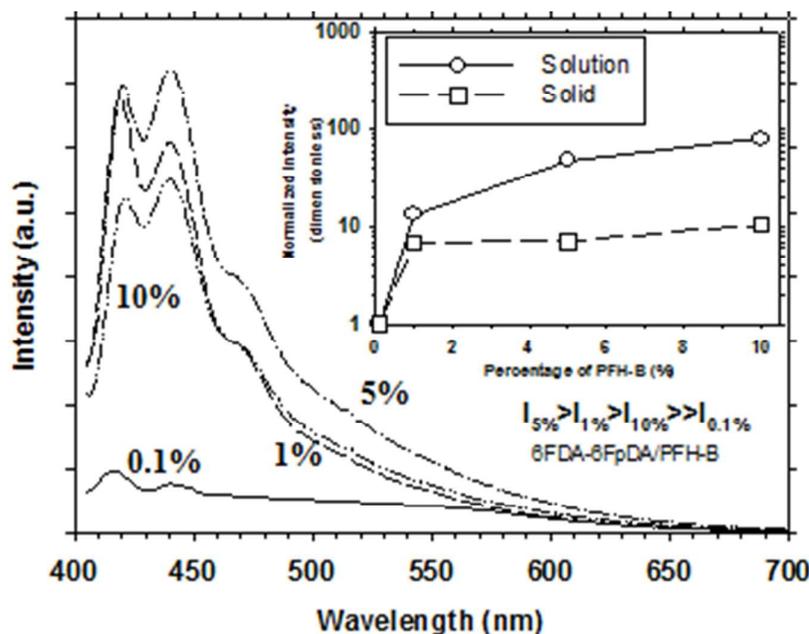Table 1. Some characteristics of the newly synthetized chemicals.

Figure 1. Synthetic approach of PFH-B, PFH-BT and PFH-NT: i) Br$_2$ /AcOH, RT, 3h (87%); ii) SOCl$_2$, Pyr, CHCl$_3$; 80°C, overnight (64%); iii) K$_2$CO$_3$, [Pd(PPh$_3$)$_4$], THF/H$_2$O, 85°C, 48h.

Figure 2. Chemical structure of the polymers used here (a) and the films obtained (b).

Figure 3. TGA curves in dynamic conditions for the blends with the highest percentage of copolyfluorene and the pure 6FDA-6FpDA without any copolyfluorene.

Figure 4. Emission spectra for 6FDA-6pDA/PFH-B films at different percentages (λ_{exc} = 390 nm). Insert: Normalized emission intensity as a function of the percentage of PFH-B in the blend.
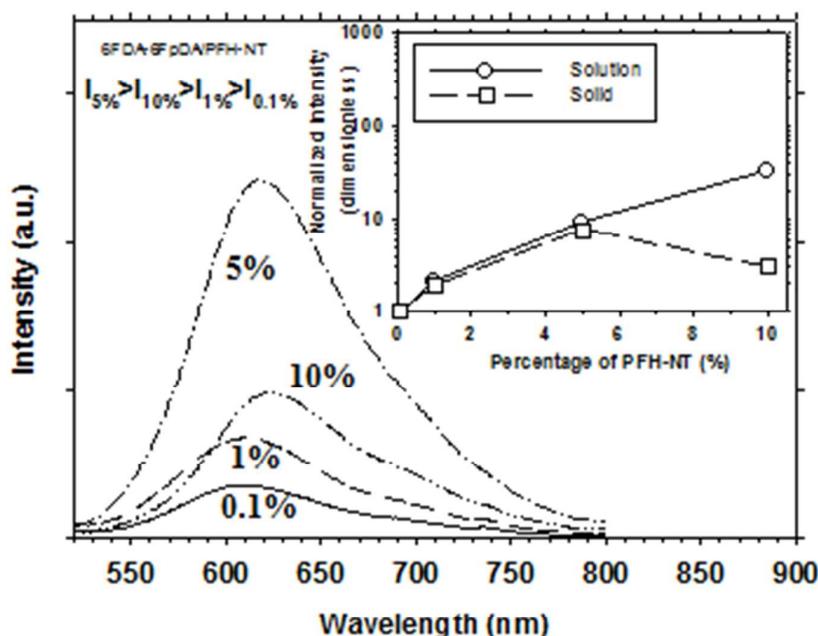
Figure 5. Emission spectra for 6FDA-6pDA/PFH-BT films at different percentages (λ_{exc} = 445 nm). Insert: Normalized emission intensity as a function of the percentage of PFH-BT in the blend.
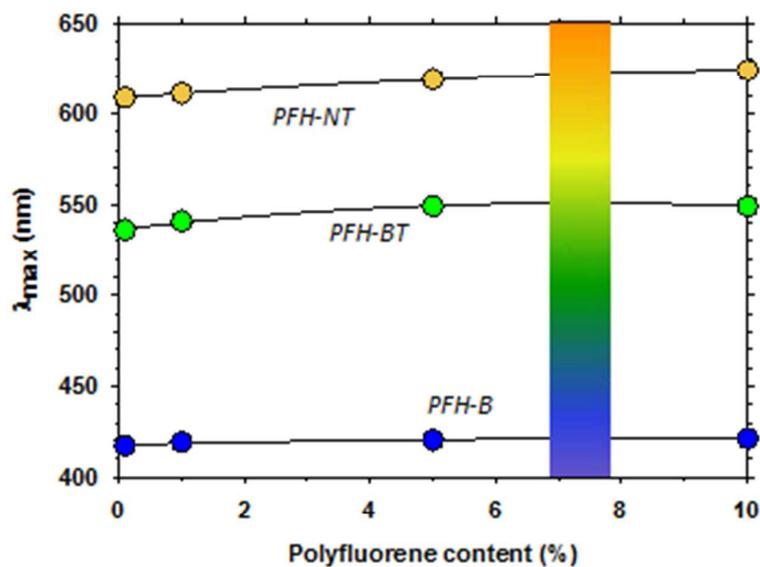

Figure 6. Emission spectra for 6FDA-6pDA-PFH-NT films at different percentages (l_{exc} = 492 nm). Insert: Normalized emission intensity as a function of the percentage of PFH-BT in the blend.

Figure 7. Redshift of the emission spectrum versus polyfluorene content.
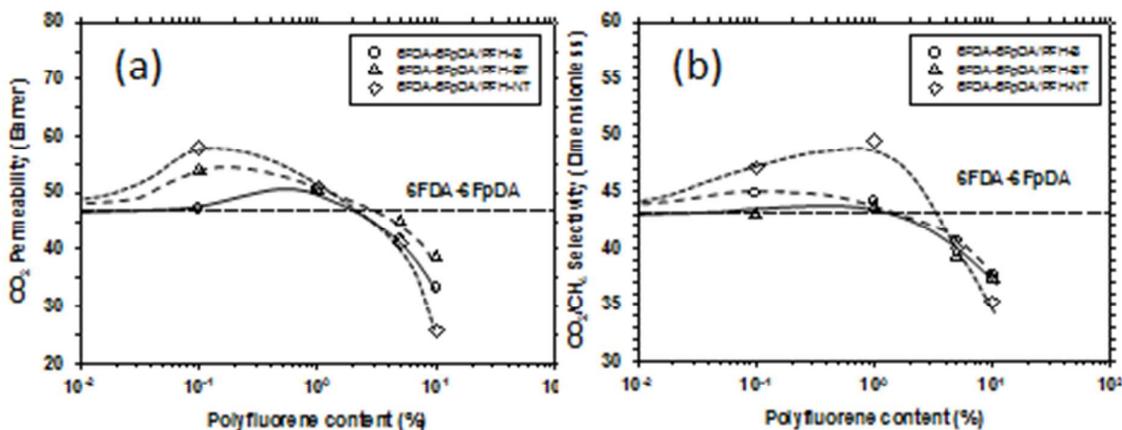

Figure 8. CO_2 permeability (a) and CO_2/CH_4 selectivity (b) as a function of the copolyfluorene in the blend. Lines are only for eye-guiding and have been extrapolated asymptotically to 0 % of polyfluorene.
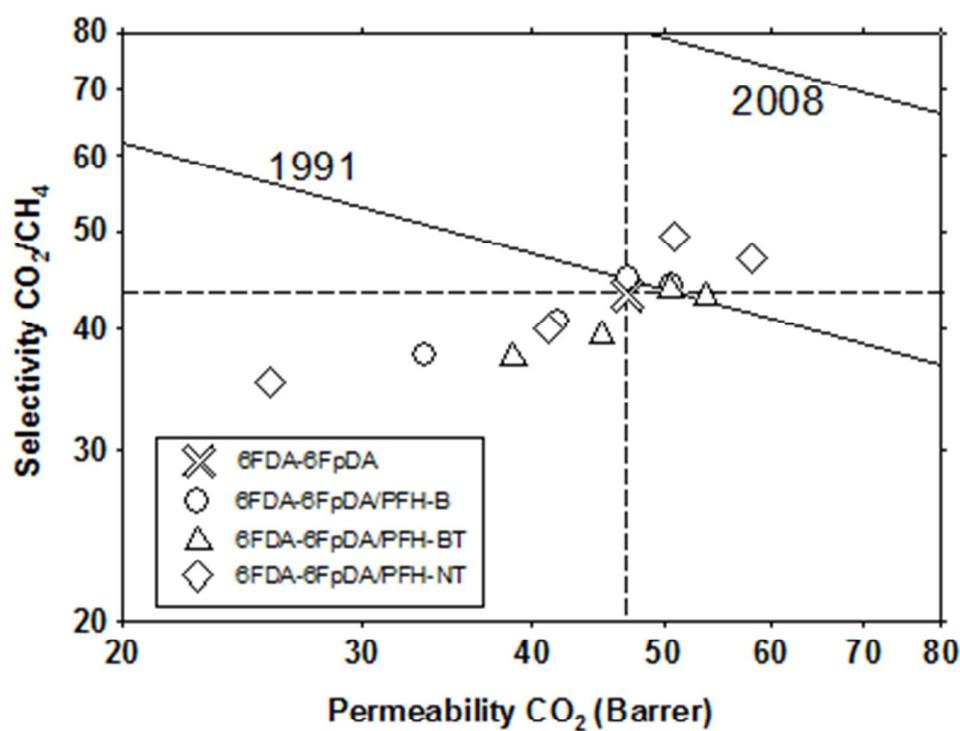
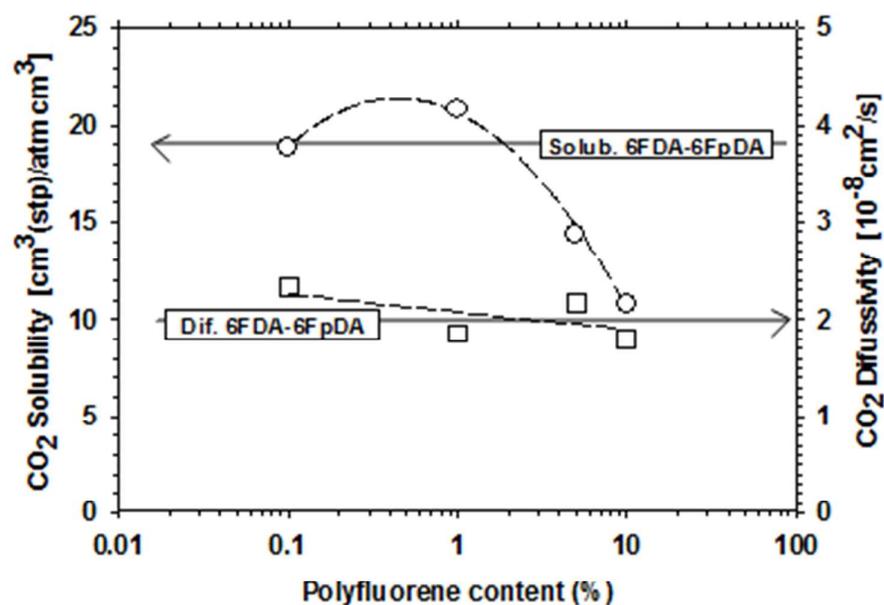Figure 9. Robeson 's plot for CO_2/CH_4.

Figure 10. CO_2 solubility and diffusivity as a function of the percentage of PFH-NT in the blends.
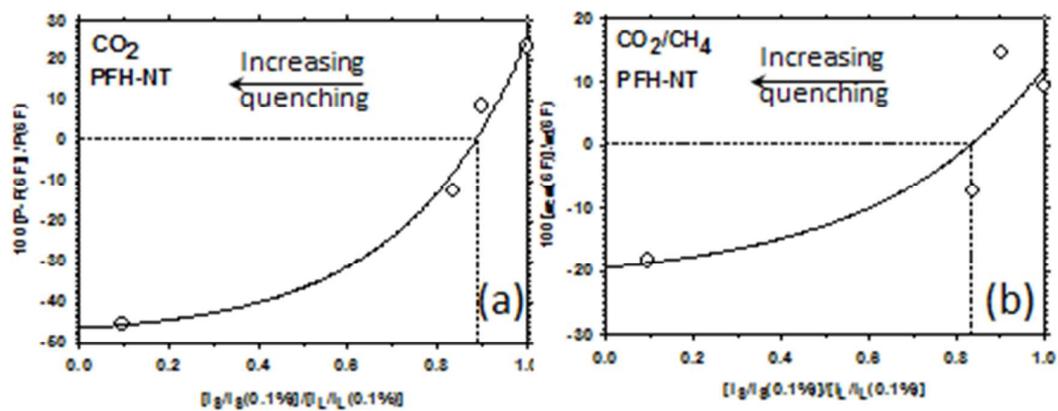
Figure 11. Percentage of increment of CO_2 permeability (a) and CO_2/CH_4 selectivity (b) as a function of fluorescence intensity in the solid state referred to that in liquid state (solid state quenching).

Table 1. Some characteristics of the newly synthetized chemicals.	
Monomers	
1,4-dibromo-2,3-diaminonaphthalene	• mp: 159-161ºC. • ^{1}HNMR (500MHz, CDCl$_3$) δ (ppm): 8.00 ("q", 2H), 7,40 ("q", 2H) and 4.27 (bs, 4H). • ^{13}CNMR (125MHz, CDCl$_3$) δ (ppm): 134.5, 127.8, 125.7, 125.0 and 106.5. • FT-IR (pellet BrK, cm^{-1}): 3423, 3380, 3347, 3267 (ν –NH$_2$), 1646 (m), 1446 (s), 1252, 752(s, ν-Napht), 703, 638, 574 and 462 (νAr-Br).
4,9-dibromonaphto{2,3}-1,2,5-thiadiazole	• mp: 237-238ºC • ^{1}HNMR (500MHz, CDCl$_3$) δ (ppm): 8.40 ("q", 2H), 7,59 ("q", 2H). • ^{13}CNMR (125MHz, CDCl$_3$) δ (ppm): 150.8, 128.9, 128.0, 123.7 and 114.3. • FT-IR (pellet BrK, cm^{-1}): 1406, 1264 (s), 1165, 892 (s), 755 (s, ν-Napht), 707, 615, 514 (s) and 448.
Copolyfluorenes	
Copoly-[9,9-bis(n-hexyl) fluorene-alt-1,4-bencene] (PFH-B)	• ^{1}HNMR (500MHz, CDCl$_3$) δ (ppm): 7.85-7.82 (m, 4H), 7.71-7.50 (m, 6H), 2.08 (4H), 1.7-1.10 (12H) 0.78 and 0.77 (2×s, 10H). • ^{13}CNMR (125MHz, CDCl$_3$) δ (ppm): 151.8, 141.0, 140.7, 140.1, 128.2, 126.8, 121.2, 120.8, 55.7, 40.6, 31.5, 29.7, 24.0, 22.6, 14.0. • GPC (polystyrene standard): Mn = 6400; Mw = 10900; PDI: 1.7.
Copoly-[9,9-bis(n-hexyl) fluorene-alt-1,4-bencene-1,2,5-thiadiazole] (PFH-BT)	• ^{1}HNMR (500MHz, CDCl$_3$) δ (ppm):8.09-7.95(m, 6H), 7.79-7.73(m, 2H), 2.15 (4H), 1.17 (12H), 0,95 (4H) and 0.80 (6H). • ^{13}CNMR (125MHz, CDCl$_3$) δ (ppm): 154.7, 151.9, 141.0, 136.6, 133.7, 133.2, 128.5, 124.1, 120.2, 55.6, 40.4, 31.6, 29.9, 23.8, 22.7, 14.2. • GPC (polystyrene standard): Mn = 2050; Mw = 4500; PDI: 2.2.
Copoly-[9,9-bis(n-hexyl)fluorene-alt-1,4-naphthalen-(2,3)-1,2,5-thiadiazole] (PFH-NT)	• ^{1}HNMR (500MHz, CDCl$_3$) δ (ppm): 8.06-7.90 (m, 6H), 7.78-7.72(m, 4H), 2.19 (4H), 1.7-1.3 (12H), 1.13 (4H) and 0.83 (6H) • ^{13}CNMR (125MHz, CDCl$_3$) δ (ppm): 154.5, 151.6, 141.2, 140.7, 138.2, 133.8, 128.5, 127.8, 124.3, 123.7, 120.6, 55.6, 40.2, 30.5, 29.5, 24.1, 22.4, 13.4. • GPC (polystyrene standard): Mn = 4500; Mw = 8600; PDI: 1.9
^{1}H and ^{13}C NMR spectra were recorded on a Bruker AVANCE 500 spectrometer, with tetramethylsilane as an internal reference. FTIR spectra were obtained using Nicolet model 520P spectrometer with samples prepared as KBr pellets. Coupled size exclusion chromatography (SEC-GPC) were carried out using an HP-1090 liquid chromatograph with autosampler, autoinjector and light scattering detector; ELSD 2200 Alltec. The size exclusion chromatogram was carried out in THF as eluent and data were calibrated using Polymer Laboratories EasiCal PS standards using two column PLGel 5 μm MIXED-C at room constant temperature.	